A Low-Noise Current Supply for an Electron Electric Dipole Moment Experiment

APPROVED BY:

_____

Daniel J. Heinzen, Supervisor

_____

Melvin E. L. Oakes, Honors Advisor

A Low-Noise Current Supply for an Electron Electric Dipole Moment Experiment

by

Daniel Borrero Echeverry

UNDERGRADUATE HONORS THESIS

Presented to the Faculty of the Department of Physics of

The University of Texas at Austin

in Partial Fulfillment

of the Requirements

for

SPECIAL DEPARTAMENTAL HONORS

THE UNIVERSITY OF TEXAS AT AUSTIN

May 2005

A Low-Noise Current Supply for an Electron Electric Dipole Moment Experiment

Daniel Borrero Echeverry

The University of Texas at Austin, 2005

Supervisor: Daniel J. Heinzen

We designed and built a custom current supply for use in an electron electric dipole moment experiment. This supply will be used to drive a set of magnetic field coils in the experimental apparatus. Based on a design used at the University of California, Berkeley in earlier electron EDM measurements, our supply sources 140mA of current with a measured noise level of $16\,nA/\sqrt{Hz}$ at 0.05 Hz, although this measurement may be too high due to the limitations of the measurement equipment. This noise level is consistent the desired level of precision ($10^{-29}\,e\cdot cm$) in the electron EDM measurement, but we believe that this noise level could be improved with further work.

Table of Contents

List of Figures

Background

The Standard Model is perhaps the greatest triumph of modern physics. It accounts for all observed phenomena and has been tested to great levels of accuracy. The Standard Model even accounts for certain time reversal asymmetries like those found in kaon decays[1]. In doing so, it puts a bound on other T-violating phenomena, one of which is the T-violating electric dipole moment (EDM) of the electron d_e. The Standard Model predicts an electron EDM of the order of 10^{-38} e·cm.[2] This level is far below the current experimental limit and is not measurable by today's technology. However, certain extensions of the standard model (most notably super symmetric (SUSY) extensions) have been proposed that predict a d_e in the 10^{-26}-10^{-30} e·cm range[3]. Multiple experiments have been performed in this sensitivity range[4,5]. The most precise of these experiments was performed by E. Commins's group at the University of California-Berkeley and set the upper bound on d_e at $1.6\text{x}10^{-27}$ e·cm. [5] Our experiment seeks to improve on this limit by two orders of magnitude by using laser cooled cesium atoms in an optical trap. Finding an electron EDM in this range would provide unambiguous evidence of new physics outside the standard model and set tight constraints on the possible alternative models. Figure 1 (below) shows the values of d_e that are permitted in a couple of these alternative models as well as the current experimental bound and our target precision. The Standard Model prediction is also shown for comparison.

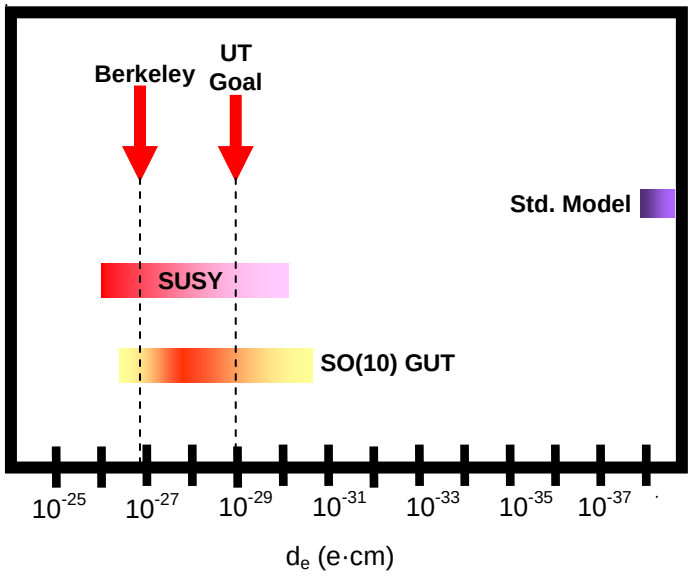

Figure 1. The electron EDM in different unified theories

Why an Electron EDM implies T-violation

If an electron had an EDM and was placed in parallel magnetic and electric fields its Hamiltonian would be given by

$$H = -\vec{\mu} \cdot \vec{B} - \vec{d} \cdot \vec{E}$$

Here $\vec{B}$ and $\vec{E}$ are the magnetic and electric fields and $\vec{\mu}$ and $\vec{d}$ are the magnetic and electric dipoles of the electron. Figure 2 shows this schematically. Every basic quantum mechanics text shows that an applied magnetic field can break the degeneracy of the energy level into separate spin states. By a similar mechanism (and substituting d for μ and E for B) a further splitting can be predicted in the presence of an electric field, as shown in Figure 3. The key characteristic is that this splitting is linear in E.

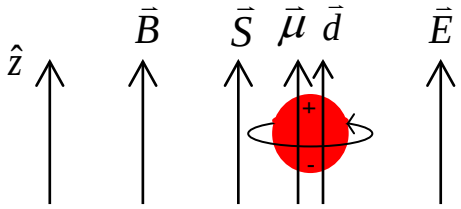

Figure 2. An electron with both magnetic and electric dipole moments in parallel electric and magnetic fields

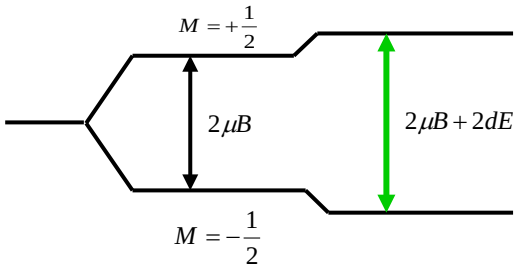

Figure 3. Line splitting due to applied magnetic and electric fields

If we now reverse time, all the currents will reverse direction and thus the applied magnetic field and the magnetic dipole moment of the electron will reverse direction as well. However, because charges are not reversed under time reversal, the electric field and the EDM are not inverted. This is shown schematically in Figure 4. Because the EDM is not reversed, the energy shift due to the electric field will be of opposite sign compared to that resulting from the magnetic field. Therefore the levels would come closer together in the case of time reversal and time reversal symmetry would be violated.

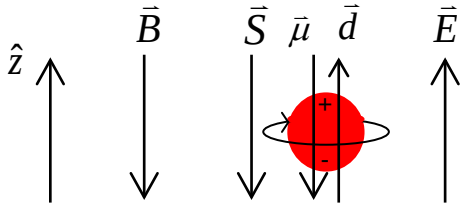

Figure 4. The same electron under time reversal

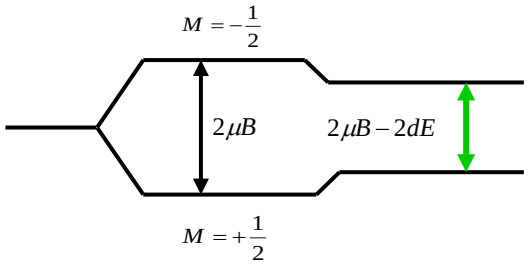

Figure 5. The line splitting is not symmetric under time reversal

T-Violation Experiment at UT

Our experiment relies on the fact that if the electron has a non-zero EDM, then an alkali atom, in our case cesium, must also have a non-zero EDM. More precisely the atomic EDM $d_a = Rd_e$, where R is called the amplification factor and is different for each element. This effect is predicted by relativistic corrections to the quantum

mechanical picture of the alkali atom that are beyond the scope of this thesis. In the case of cesium, the amplification factor has been calculated to be 120 [6]. By measuring the characteristic linear shift in the atomic levels with an applied electric field, we hope to measure the electron EDM with great precision.

The novel aspect of our approach is that the atoms will be held in an optical dipole force trap[7] (FORT)[*], thus eliminating the major sources of error that have limited previous experiments. These experiments have used atomic beams and have therefore been susceptible to $\vec{v} \times \vec{E}$ effects. Such effects arise because in their rest frame the atoms see a motional magnetic field $\vec{B}_{motion} = \frac{\vec{v}}{c} \times \vec{E}$, which gives a line shift that is linear in E (for a fixed angle between $\vec{v}$ and $\vec{E}$) and can be confused with the signature linearity of EDM splitting. Previous experiments have corrected for this but have probably reached their technical limit. Our design has the added advantage that because they are trapped, the cesium atoms in our experiment can be probed for much longer periods of time than those in the beam experiments. This reduces statistical error and gives narrower line widths. The trapping also helps deal with field inhomogeneities because the atoms are spatially localized throughout the measurement.

Below (Figure 6) is a schematic representation of our experimental apparatus. Atoms are shot into our apparatus using a 2-D Magneto-Optical Trap (MOT) that confines the atoms in two dimensions, thereby shooting them out along the third[8]. Once the atoms enter the test chamber, they are slowed down with optical molasses[9]. Some of these slowed atoms will then fall into one of FORTs. Three conducting plates separate the two FORTs. These plates provide an applied electric field E of 100kV/cm. Because of this atoms and not individual electrons the obvious choice for our experiment, as electrons would immediately be accelerated out of the traps by such an electric field. A set of magnetic field coils provides the magnetic bias field B. The whole thing is placed in ultra-high vacuum to prevent trap loss due to collisions with the background gas and to prevent arcing across the electric field plates.

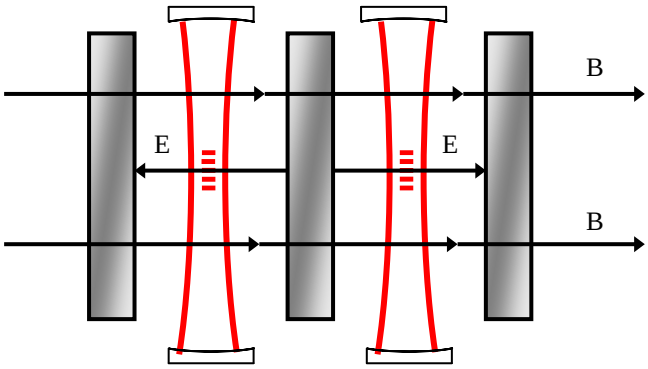

Figure 6. The experimental test chamber

[*] The perturbations to the atomic levels due to the trap can be made very small and should be a manageable source of error.

Magnetic Field Noise

Even though it removes many sources of error, it turns out that our experiment also has its own limiting sources of error. One of the most important is magnetic field noise. Because any EDM splitting will be observed in the presence of magnetic fields, any magnetic field noise will translate into uncertainty in the EDM measurement. In particular, there are three main sources of magnetic noise. The first is noise generated by Johnson currents and residual magnetism in the metallic elements of the apparatus. The second is background noise from the Earth's magnetic field and from electronic devices in our lab. The last and most important for our purposes is noise in the magnetic bias field.

The uncertainty in the magnetic field splitting leads to an uncertainty in the electric splitting given by the following:

$$\mu_B \delta B = \delta d_e RE$$

Here, δB is the uncertainty in the magnetic field and δd_e is the resulting uncertainty in the electron EDM measurement. The RMS uncertainty is given by $\delta B_{rms} = \sqrt{S_B(\nu)} \big/ \sqrt{T}$, where $S_B(\nu)$ is the spectral noise density in G^2/Hz, ν is the modulation frequency, and T is the total measurement time. We define the magnetic field noise to be $B_{noise} = \sqrt{S_B(\nu)}$. Thus, in order to achieve δd_e of $10^{-29} e \cdot cm$, we would require the magnetic field noise to be less than $6.5 \times 10^{-12} G/\sqrt{Hz}$.

This requirement was felt to be too stringent, and therefore we added a second measurement region. By measuring the difference in the Zeeman splitting in the two regions, we can reduce the uncertainty by a factor of two, at the expense of additional considerations. It is virtually impossible to guarantee a field in that is exactly the same in both regions. This can be corrected by switching the plate polarities at regular intervals ($\tau \sim 10$ s), thereby modulating the signal at around 0.05 Hz. When the electric field in the first region is parallel to the magnetic field the line splitting is given by

$$\frac{3}{2}\mu_B B_1 + \frac{3}{2} d_e R E$$

where B_1 is the magnetic field in the region. Accordingly, the splitting in the second region is given by:

$$\frac{3}{2}\mu_B B_2 - \frac{3}{2} d_e R E$$

Here B_2 is the magnetic field in the second region. Subtracting the splitting in the second region from the splitting in the first, we get:

$$\left(\frac{3}{2}\mu_B B_1 + \frac{3}{2} d_e R E\right) - \left(\frac{3}{2}\mu_B B_2 - \frac{3}{2} d_e R E\right) = \frac{3}{2}\mu_B (B_1 - B_2) + 3 d_e R E$$

When the electric field reverses, we again measure the line splitting and we get:

$$\left(\frac{3}{2}\mu_B B_1 - \frac{3}{2}d_e R E\right) - \left(\frac{3}{2}\mu_B B_2 + \frac{3}{2}d_e R E\right) = \frac{3}{2}\mu_B (B_1 - B_2) - 3d_e R E$$

We then subtract the two results, thereby isolating the EDM signal, as follows:

$$\left[\frac{3}{2}\mu_B (B_1 - B_2) + 3d_e R E\right] - \left[\frac{3}{2}\mu_B (B_1 - B_2) - 3d_e R E\right] = 6 d_e R E$$

This procedure allows us to bypass the problem of having exactly equal fields in both regions and makes us sensitive only to the effects that affect the difference in the magnetic field between the two regions, B_1-B_2.

One such effect has to do with the proximity of metals to the atoms being probed. This is due to the fact that the metals traditionally used in high vacuum systems become magnetized when exposed to a magnetic field. Such magnetization can lead to field inhomogeneity within the experimental apparatus, which is not a problem as long as it is constant in time. However, as the electric field plates charge, the charging currents can create magnetization that is correlated with the electric field reversal, thus generating a false EDM signal. This effect renders stainless steel unusable for our application, so we are forced to resort to using titanium, which is much less magnetic, for the construction of our chamber.

There is another noise mechanism that is related to the use of metals called Johnson currents. Johnson currents occur because the thermal motion of electrons inside a metal generates minute currents in the conductor. Of course the average current is zero, but the instantaneous currents generate small magnetic fields. This noise mechanism is most evident in close proximity of the conductive surfaces and drops off quickly with distance. This means that the noise in each region is uncorrelated to that in the other region, so that this mechanism must be evaluated in the single region limit. Even titanium is too noisy to be in close proximity of the trapped atoms, so we resorted to conductively coated glass to build the electric field plates. Calculations have shown that such plates will generate about $5\times10^{-12}\, G/\sqrt{Hz}$ of white noise. We can also expect $\sim 10^{-12}\, G/\sqrt{Hz}$ of noise due to Johnson currents in the vacuum can. Our chamber design maintains other conductors as far as possible from the test regions, thus keeping the noise level below the single region limit.

Another source of magnetic noise is the background noise from the lab. In order to prevent background noise from affecting our measurement, the whole experimental apparatus will be enclosed in five concentric magnetic shields. Made of Mu-Metal, a nickel-iron alloy, these shields use their very high permeability to deflect magnetic fields. Calculations by M. Kittle have shown that five concentric cylindrical shields could reduce background noise by a factor of up to 2 million.

The noise source most relevant to this thesis comes in the form of current noise in the bias field coils. The magnetic field generated by the current going through the coils is given by

$$B = f_{geometric}\, I$$

Here $f_{geometric}$ is a proportionality factor that is dependent on the geometry of the field coils[*] and can be calculated using the Biot-Savart Law for a given coil geometry. Because the magnetic field coils for our apparatus have not been designed yet, the exact value of $f_{geometric}$ cannot be calculated explicitly. However, since we know the magnetic field we want (1mG[**]) and we know the current that is supplied by our current source (140 mA), we can calculate that $f_{geometric}$ should be around 7.14 mG/A.

Unlike the noise produced by Johnson currents, background and bias fields are very homogenous. Therefore, our real concern is not with the homogeneity of the field but with stability of its spatial distribution, which can be quantified by the spatial derivative B′. B′ can be approximated by B/L, where L is the distance over which the magnetic fields vary. While L is yet to be determined, it should be much larger than the distance between the measurement regions and a reasonable estimate is around 100 centimeters.

With this in mind, the above relation becomes

$$\mu_B \delta B' D = 2\delta d_e RE$$

The factor of two accounts for the decrease in uncertainty obtained by using two measurement regions and $\delta B' D$ is the first order approximation of the uncertainty in the magnetic field over the traps. Here $\delta B' = \delta B / L$ is the uncertainty in the magnetic field gradient and D is the distance between the two traps. Substituting from the equations above and solving for B_{noise}, we get

$$B_{noise} = \delta d_e \frac{2RE L\sqrt{T}}{\mu_B D}$$

If we plug in the parameters of our system (R = 120, E = 10^5 V/cm, T = 10^5 s, L = 100 cm, and D = 1.5 cm) and set the desired δd_e of 10^{-29} e·cm, we find that our magnetic field must have less than $8.75\times10^{-10}\, G/\sqrt{Hz}$ at 0.05 Hz. We will now examine the sources of magnetic noise more closely, keeping this requirement in mind.

Measurements of the lab's magnetic background by Kittle and T. Burton have found it to be less than $1\times10^{-4}\, G/\sqrt{Hz}$ at 0.05 Hz. Because our shields will have several

[*] The construction of the coils themselves can be a source of noise. In order to for $f_{geometric}$ to remain constant, the coils must be constructed in such a way that their geometry remains constant (ie. they are dimensionally stable).

[**] 1 milliGauss was chosen as compromise value. This is the compromise between the difficulty of suppressing the noise in a larger field and the inadequate error suppression of a smaller field. These other errors arise when using the Ramsey method to probe the atoms.

holes in them in order to feed through the trapping and probing lasers, vacuum pumps, and the high voltage supply for the electric field plates, we can assume that they will be less effective than the ideal. Using a reduced shielding factor of 500,000 to account for this, we can expect that the magnetic background noise to be attenuated to less than $2\times10^{-10}\ G/\sqrt{Hz}$ at 0.05 Hz, which is below our required two-region limit.

Subtracting this expected residual background noise from the maximum desired noise level, we can now set a constraint on the current noise permissible in our coils using the expression we derived in our discussion of the bias field noise, such that

$$I_{noise} \le B_{noise} / f_{geometric}.$$

For the desired level of magnetic field noise this gives us a maximum noise current of $119\,nA/\sqrt{Hz}$ at 0.05Hz.

Design

Current Source

Because the experiment is so sensitive to magnetic field noise, the magnetic bias field must be as constant as possible. In order to achieve this, the bias coils must be supplied with a constant current. Unfortunately, no commercial current source exists that can provide the required precision (at least at the low frequencies required), but individual components can be purchased and assembled in such a way that they are stable enough for the application. We began our design with a circuit designed at the University of California at Berkeley in 1993. [10] This design is shown in Figure 7 below.

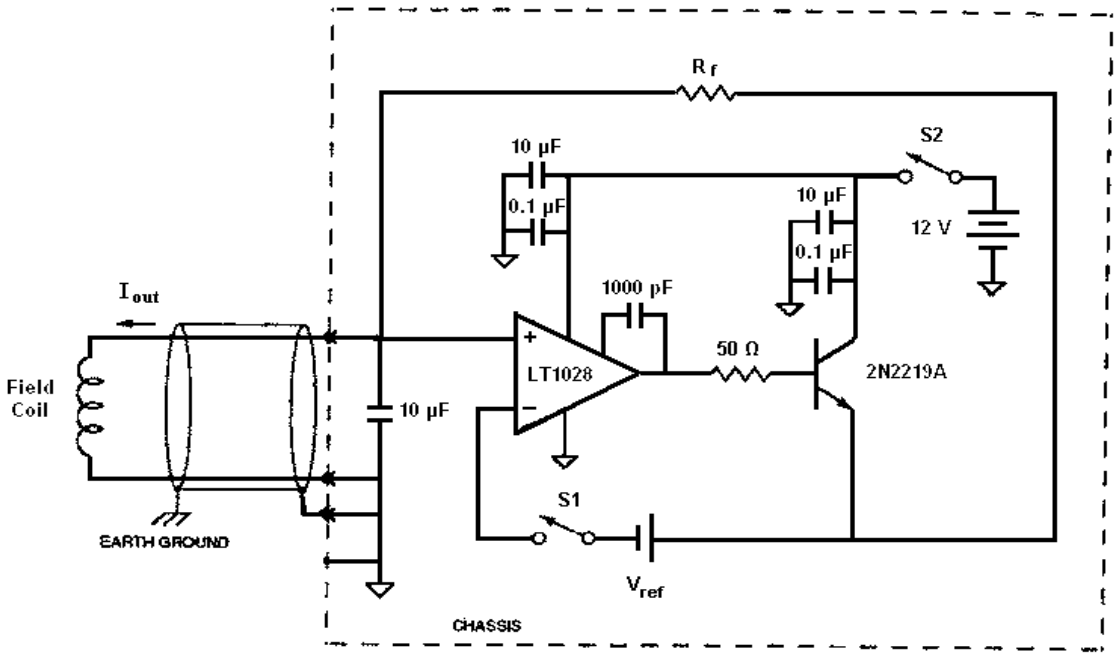

Figure 7. Current supply circuit

This circuit design uses a transistor to control a constant current draw from a C&D Technologies BBG-180RT 12 Volt Gell-Cell battery. Such batteries are optimized for continuous current drain and operation in a broad range of temperatures[11]. The amount of current drawn is controlled by a high-precision LT1028 operational amplifier, which compares the voltage drop across the current sensing resistor R_f to a stable reference voltage V_{ref}, while introducing only a mere 12 $nV/\sqrt{Hz}$ of voltage noise at 0.5 Hz[12]. Because of the feedback in the circuit, the op-amp's two inputs are at the same voltage, so the voltage drop across R_f exactly cancels V_{ref}. Therefore, we have $V_{ref} + IR_f = 0$ and solving for I, we get that $I = -V_{ref}/R_f$. Due to the op-amp's large input impedance, all the current that flows through R_f must also flow through the field coils to ground. Therefore,

$$I_{out} = \frac{V_{ref}}{R_f}$$

Hence, the stability of the output current depends almost exclusively on the stability of V_{ref} and R_f, but also on Johnson noise, shot noise, and any noise added by the LT1028.

Some modifications to Berkeley circuit were necessary. The original design used a 1.35V E401N mercury cell as the reference voltage. Unfortunately, mercury cells are no longer readily available due to ecological concerns. Preliminary tests by S. Whitney and T. Burton, two former members of our group, showed that the silver-ion, zinc-air, and alkaline replacements are too noisy for the application. Luckily, Linear Technology produces an IC reference, the LTZ1000 ultra-precision reference[13], which has been shown to have not only an extremely low noise signature ($460\,nV/\sqrt{Hz}$ at 0.5Hz), but also long term drifts as low as a few ppm/year.[14] The LTZ1000 uses a temperature compensated, subsurface Zener diode to provide a 7V reference voltage that has been successfully used in many high precision applications including as a Volt standard aboard NASA's SORCE mission[15] and by the Standards Laboratory at CERN[16]. However, the implementation of the current supply using the LTZ1000 required some special care.

The first issue that we had to deal with was the fact that the LTZ1000 requires an external power supply and outputs its 7 volts of reference voltage above the supply ground. Using a traditional regulated power supply would mean that the negative terminal of the reference would in some way be tied to Earth ground. This also happens to be the circuit ground for the current supply circuit. In the worst case, the negative terminal of the reference to be at Earth ground and the current supply circuit could not possibly work properly. In any case, any tie to Earth ground, even an indirect one, could cause all sorts of problems, so we avoided this by floating the reference circuit by powering it from a separate DieHard Deep Cycle 12V lead-acid battery.

Using the LTZ100 increased the reference voltage by a factor of 5 from the original 1.35V. If we had used the resistance value of R_f used in the original design

(10Ω), I_{out} would also have increased by a factor of 5 to around 700mA. Not only is this very close to the maximum collector current rating for the 2N2219A transistor[17], but it also drains the supply battery unnecessarily. Therefore, we scaled R_f up in proportion to the voltage increase. By setting R_f to 50Ω, we achieve an output current of around 140mA, which is smaller than 700mA but still sufficiently large to drive the bias coils.

The fact that the LTZ1000 puts out 7V also reduces the range of possible loads that can be applied to the circuit. This happens because the non-inverting input of the op-amp is floating at $V_L = I_{out} R_L$ above circuit ground, where R_L is the load resistance. While this is an advantage in the sense that the same amount of current is sourced regardless of any drift in the circuit ground, it also plays a limiting factor in the circuit operation. Following the standard op-amp rules, the inverting input is also at V_L, and therefore the transistor emitter is at $V_E = V_L + V_{ref}$. In order for the circuit to work, the transistor must be forward biased, so that V_E cannot exceed 12V. For the present value R_f (and consequently I_{out}), this limits the maximum load resistance that can be successfully supplied by the current source, without risking malfunction. This maximum value can be estimated as follows:

$$V_E = V_{ref} + V_L = V_{LTZ1000} + I_{out} R_L \le 12V .$$

Therefore,

$$R_L \le \frac{12V - V_{LTZ1000}}{I_{out}} = \frac{12V - 7V}{140mA} \approx 35\Omega$$

To ensure proper operation, special care must be taken when designing the bias field coils not to exceed this load limit.

Vishay VHP-3 Bulk Metal Foil Current Sensing Resistor

In order to obtain maximum current stability, R_f must be extremely stable. This is achieved by using a Vishay VHP-3 current sensing resistor[18]. Constructed by cementing a Nichrome foil to a planar ceramic substrate, bulk metal foil resistors like the VHP-3 are carefully constructed to minimize thermal sensitivity. Using this proprietary technology the VHP-3 can obtain temperature coefficients of resistance as low as 2 ppm/^{o}C and long term stability better than 0.01% over 2000 hours, even while dissipating 3 Watts of power. In the case of our 50Ω VHP-3, this works out to be a mere 100 μΩ/^{o}C and less than 0.5Ω over the lifetime of the experiment[*].

Two intrinsic noise sources are associated with any resistor. These are Johnson or thermal noise and shot noise and are present independent of the specifics of the resistor's construction. Johnson noise arises from the thermal motion of the electrons in the resistor and independent of applied voltage. Because the thermal motion of the electrons is random, sometimes more electrons will be in one end of the resistor than on the other,

[*] One might even expect a smaller drift because our resistor will only be required to dissipate around 1W.

resulting in a voltage drop, and if the circuit is closed in current noise. Naturally, the time-averaged value of such a current is zero, but instantaneously this is seen as white noise given by:

$$I_J = \sqrt{\frac{4kT\Delta\nu}{R}}$$

Here k is Boltzmann's constant, T is the absolute temperature of the resistor in Kelvin, R is the resistance, and $\Delta\nu$ is the bandwidth of the system. Dividing through by $\sqrt{\Delta\nu}$ and plugging in T = 300 K (our resistor runs slightly hotter than room temperature) and R = 50 Ω, we get that the Johnson noise in the VHP-3 is around $20\ pA/\sqrt{Hz}$.

The second intrinsic noise mechanism is shot noise. Shot noise occurs because the charge carried in a current is quantized. The exact number of electrons going through the resistor at any given time is not constant but fluctuates and this shows up as white noise given by:

$$I_S = \sqrt{2eI_{DC}\Delta\nu}$$

Here e is the charge of the electron, $\Delta\nu$ is the system bandwidth, and I_{DC} is the DC current through the resistor. For I_{DC} = 140 mA, this corresponds to $0.2\ nA/\sqrt{Hz}$.

Additionally, the VHP-3 design introduces a voltage noise of less than 10 nV per volt of applied voltage[*]. In our case this works out to a maximum of 70 nV, which corresponds to a current noise of 1.4 nA. The VHP-3 also guarantees a low temperature coefficient of 0.1μV/ ^{o}C, which corresponds to a current noise of around 2 nA/^{o}C and is better than we can expect from the LTZ1000 voltage reference. This turns out to be the most sensitive aspect of resistor and for this reason the circuit is built in a box filled with Styrofoam packing peanuts, which help provide thermal stability. We can expect the VHP-3 to introduce a maximum of about 2.5 nA of current noise, although it should probably be less[**].

The robust construction of the VHP-3 also has one additional advantage. Because it has a relatively thick Nichrome foil (25,000Å), the VHP-3 is much less susceptible to damage from humidity than its equivalent thin film counterparts. However, this is not critical in the air-conditioned environment of our lab.

[*] This number is given in the VHP-3's datasheet noting that 10nV/V is the limit of their testing equipment. No spectral distribution is given for this noise mechanism. It is also unknown whether this figure includes Johnson noise.

[**] 2.5 nA was calculated using the maximum design noise of 1.4 nA and assuming temperature stability of about 1^{o}C.

Linear Technology LTZ1000 Ultra-Precision Reference

The other necessary element for a stable output current is a stable voltage reference. The LTZ1000 is an ultra-stable voltage reference manufactured by Linear Technology. It has two major components that make it the most stable commercial reference available[**]. The first is a buried Zener reference, which provides the reference voltage, and the second is a temperature sensing heater, which stabilizes the substrate temperature. Its superior precision comes at the cost of substantial external circuitry that must be used to set its operating currents and bias voltages. We will first discuss the reference circuit and follow with a discussion of the temperature stabilization circuit.

The reference circuit consists of a buried Zener diode and a temperature-compensating transistor (both of which are built into the LTZ1000 package) along with two external resistors, a filtering capacitor, and an LT1013 operational amplifier. Because it is buried below the surface of the silicon, the buried Zener is able to avoid the oxidation and contamination problems that make regular Zener diodes practically useless as precision references. The reference circuit schematic is shown in Figure 8.

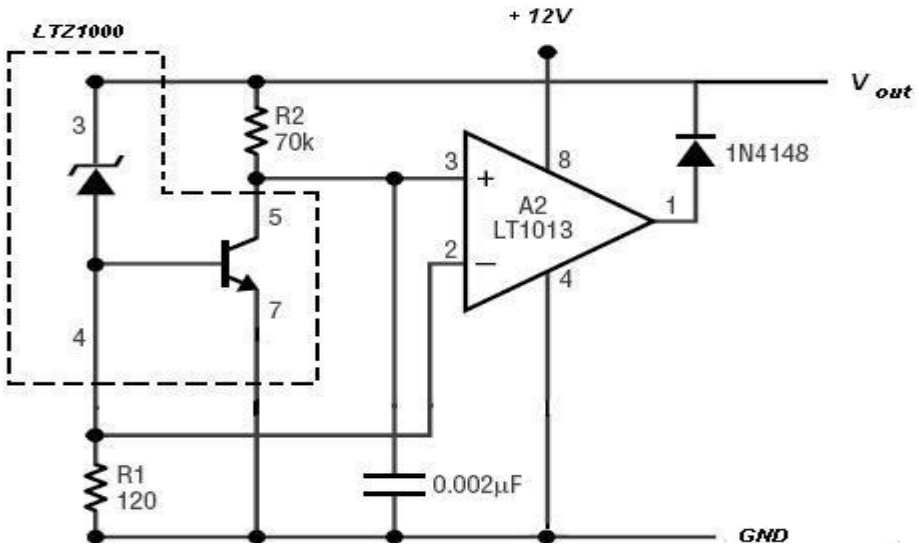

Figure 8. Voltage Reference circuit diagram

When the circuit is turned on, the op-amp tries to set the base-collector voltage of the transistor to zero. In doing so, it sources a current that reverse biases the Zener diode. The Zener acts like a variable resistor that adjusts its resistance to always drop a voltage V_Z of around 6.5V. Because of the feedback loop, the op-amp sets the transistor collector voltage equal to the Zener anode voltage and in doing so applies a voltage across R2. A small current then flows through R2, such that $I_C = V_Z/R2$. For R2 = 70kΩ, the collector current is around 100 μA. Because the op-amp's input impedance is very large, the current is forced to flow through the transistor (with the AC components shorting to

[**] Superconducting Josephson junction standards provide a more stable reference but require cryogenic cooling. Weston cell standards are also more stable but are not very portable and have high temperature coefficients.

ground via the bypass capacitor), and as it flows through the base-emitter junction, the junction acts like a forward biased diode dropping around 600 mV. Thus, the overall reference voltage is given by V_Z + 600mV = 7.1V. The voltage across the base-emitter junction is also the voltage across R1 and results in a current of 5 mA. This current must come thru the Zener, and thus R1 sets the Zener bias current*. The reference noise decreases for greater bias currents but the lifetime of the Zener is reduced, so 5mA is a good compromise value.

The temperature-compensating transistor actually serves a dual purpose in the reference. By itself, the Zener has a relatively high temperature coefficient of about +2mV/^{o}C, which is clearly unacceptable in this application. But because the base-emitter junction of the transistor has a temperature coefficient of roughly -2mV/^{o}C, putting the junction and the Zener back to back reduces the total circuit temperature coefficient to almost zero[19].

Because the temperature coefficients of the transistor and the Zener do not exactly cancel, the LTZ1000 uses an onboard heater to maintain the substrate at a constant temperature. The heater is powered by a 2N3904 transistor, which is controlled by minute changes in the base-emitter voltage of a temperature-sensing transistor. The schematic for this part of the circuit is shown in Figure 9 below.

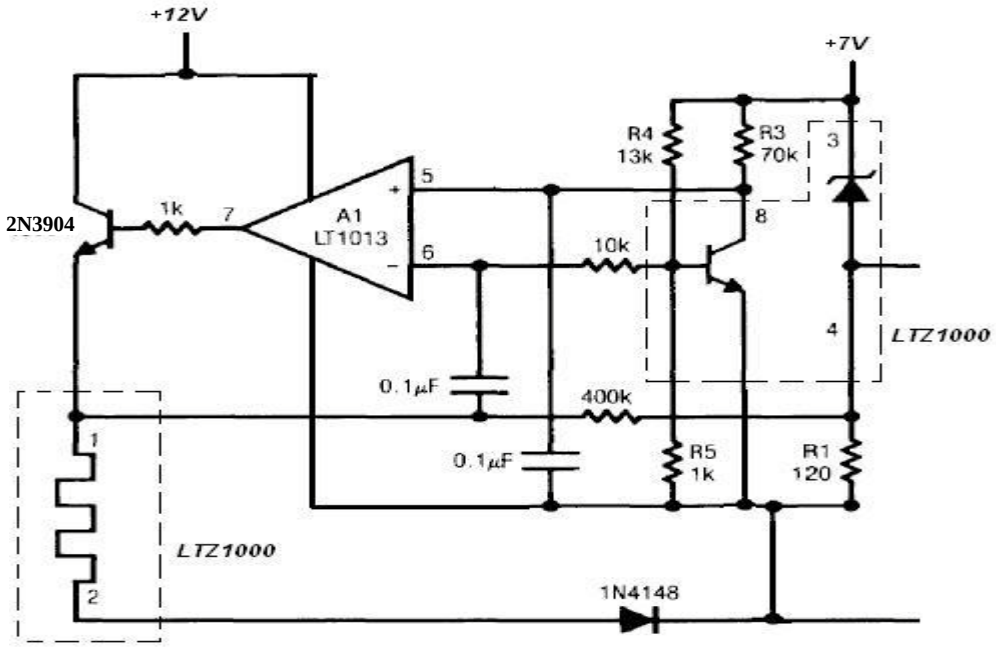

Figure 9. LTZ1000 Temperature Control

* Naturally a part of the bias current flows into the transistor base but this is negligible because the base current is smaller than the collector current by a factor of h_{FE}, which is around 200 for this transistor. Therefore, the base current is only around 0.5 μA.

As before, the transistor collector current is set by R3. R4 and R5 act as a voltage divider and their values are set so that the base-emitter voltage corresponds to the base-emitter voltage at the desired temperature setting[20]. In our case, we use R4 = 13kΩ and R5 = 1kΩ, so that the base-emitter voltage is around 500mV. This corresponds to an operating temperature of around 60°C. Roughly speaking a change of 0.5kΩ in R4 will change the operating temperature by about 5°C. In order to maintain a constant temperature, precision metal film resistors were used for R4 and R5.

If the chip heats up above the set temperature, the base-emitter voltage will decrease by 2mV/°C. Accordingly, the collector voltage will also drop, as more current is drawn through R3. This drop will be amplified by the LT1013 op-amp*, reducing the base current of the power transistor, and hence reducing the power dissipated in the heater. The complete LTZ1000 circuit puts these two circuits together and is shown in Figure 10. The positive reference terminal is at $+V_{ref}$ and the negative terminal is at ground. Because the heater is inherently noisy, special care must be taken to make sure that the heater current has its own return path to ground that is separated from the voltage reference ground.

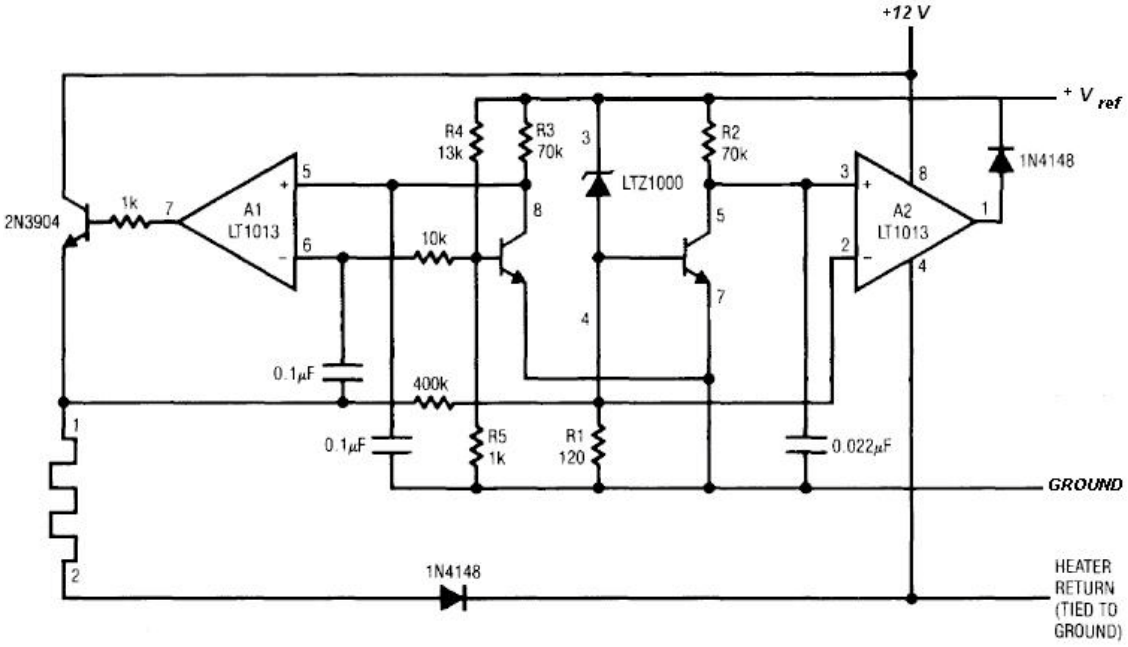

Figure 10. Temperature Compensated Low Noise Voltage Reference

* The op-amp inputs are both have bypass capacitors to eliminate AC components of the control signals.

Construction

The circuits discussed above were constructed on 2oz. single sided PC board using SWG 22 solid core wire to make all the connections. Rosin core tin/lead (60/40) solder was used. The circuit was kept small (3in x 3in) to minimize thermal gradients across the board. Heat sinks were mounted directly on the VHP-3 resistor and the 2N2219A transistor in the current supply circuit. The whole circuit was put in a metal box that was filled with Styrofoam packing beads to maintain thermal insulation. Precision metal film resistors and capacitors were used throughout to minimize noise[21]. External connections were made using coaxial cable with the braid grounded or cables with aluminum foil shielding. The complete circuit diagram is shown in Figure 11. **For more construction details see Appendix A.**

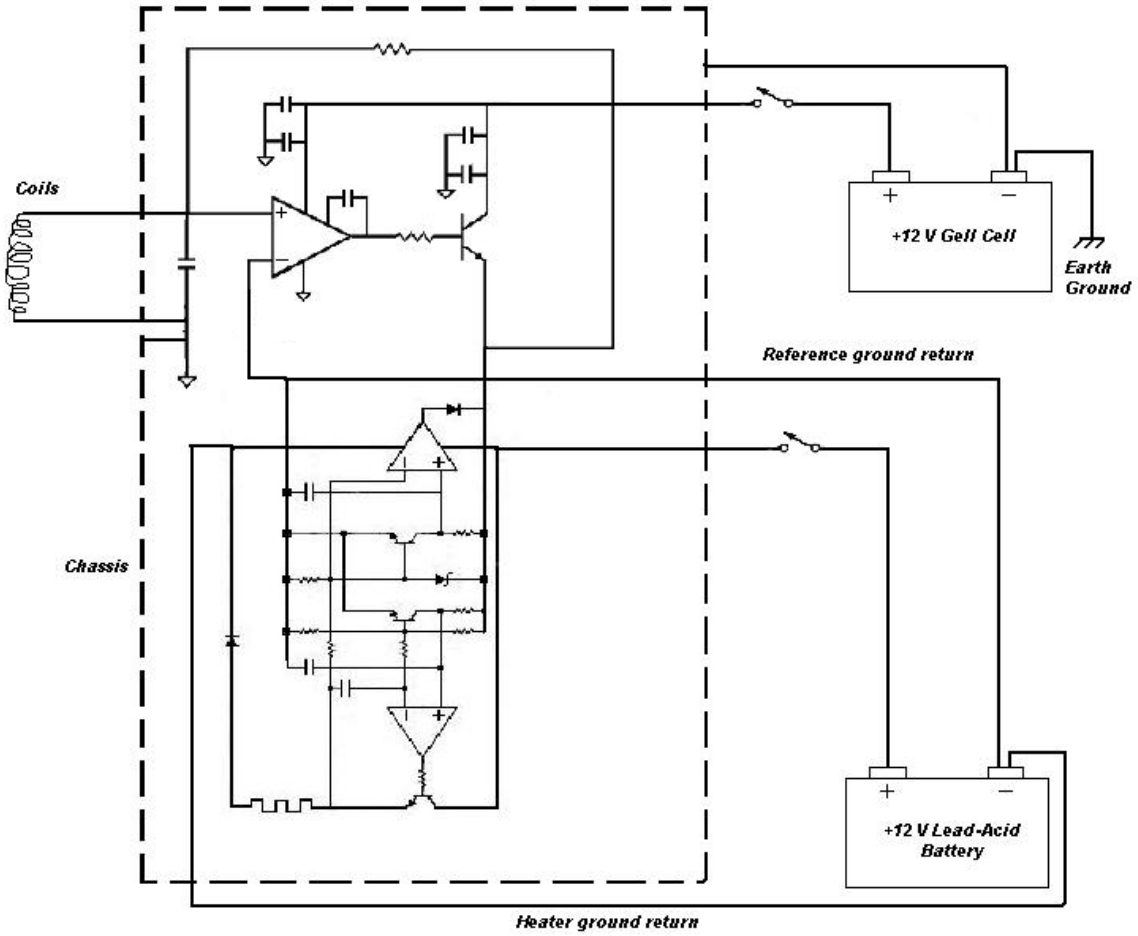

Figure 11. Complete current supply circuit diagram

Noise Measurement

Having constructed the current supply, the next step was to measure the current noise in its output. This was in two steps. First, we measured the voltage noise directly on the LTZ1000. This was done to ensure that it was working properly. Next we measured the noise on the current by measuring the voltage across R_f. Both voltages were measured differentially on a Stanford Research Systems SR560 Low Noise Preamplifier, which was AC coupled and filtered for frequencies above 3 Hz. The SR560 was set to a gain of 10,000 in its low noise setting (i.e. more gain is allocated toward the front end to elevate small input signals above the amplifier noise floor[22]). In this setting the SR560 introduces $270\,\mathrm{nV}/\sqrt{\mathrm{Hz}}$ of noise at 0.05 Hz[*]. All connections were made using shielded BNC cables. Figure 12 shows the measurement setup.

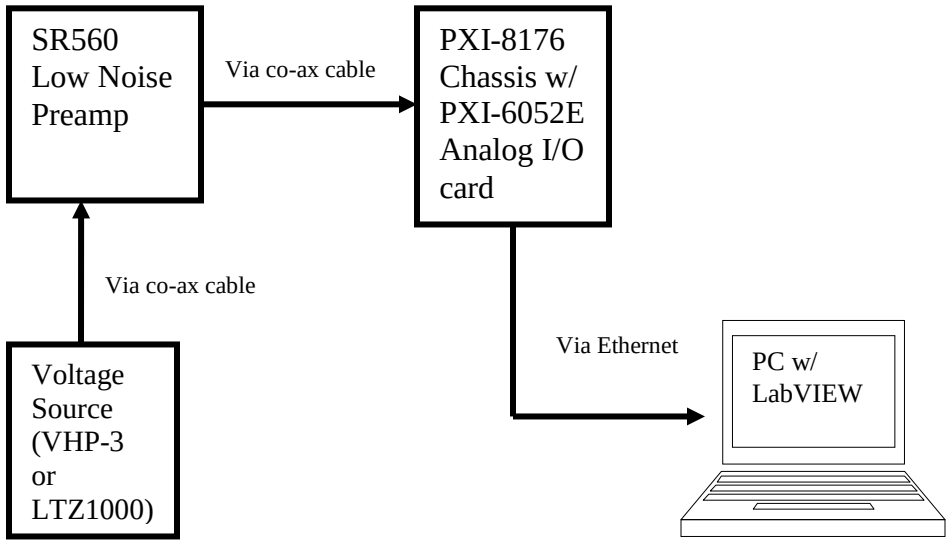

Figure 12. Voltage Measurement Setup

The amplified signal was then acquired using a National Instruments PXI-6052E Analog Input/Output DAQ Card using a LabVIEW script. The script was run remotely in a PXI-8176 Embedded Controller. The block diagram for this script is shown in Figure 13. It makes use of the Spectral Measurements and Write LVM Express VI's provided by National Instruments and was put together using mostly pieces of sample code provided in the LabVIEW examples. The measurements were automatically scaled to remove the amplifier gain.

[*] Stanford Research Systems does not give noise information below 1 Hz. Therefore, we extrapolated their noise curve using a 1/f fit.

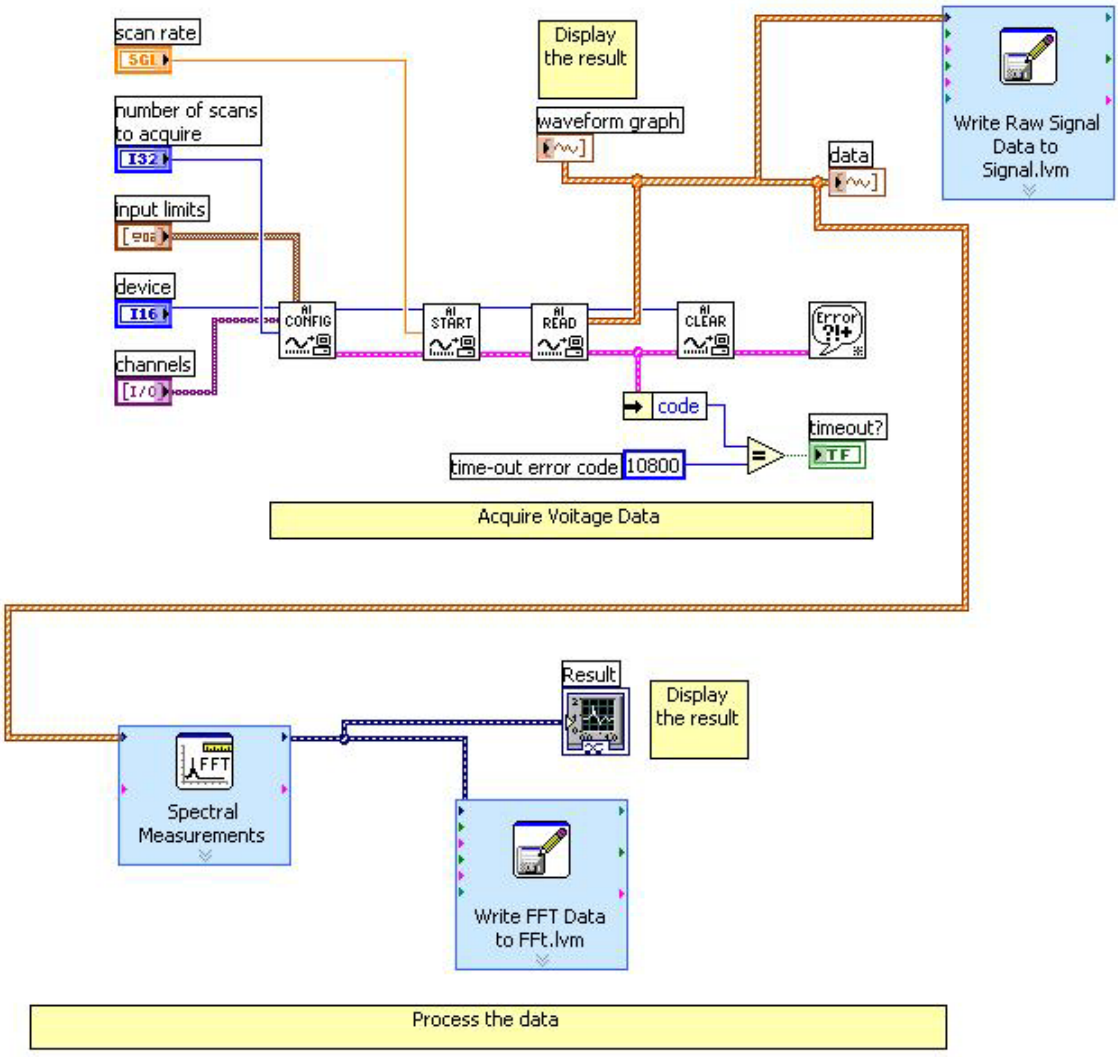

Figure 13. LabVIEW Data Acquisition and Processing Script

Results

We first measured the voltage noise directly on the LTZ1000. One minute worth of data is shown for reference in Figure 14. Data was gathered over an hour at 20 samples per second and then the noise spectral density was calculated using the Spectral Measurements Express VI provided with LabVIEW. The voltage noise is given by the square root of the spectral density. Figure 15 shows the noise spectrum of one hour's data. Also shown for comparison are the noise spectrum of a 1.5 alkaline battery and a reconstruction of the LTZ1000 noise spectrum given by the manufacturer. It is immediately obvious that the LTZ1000 is superior to the alkaline battery. It is also apparent that we could not accomplish the noise level that the manufacturer advertises. By extrapolating the noise spectrum curve given by Linear Technology, we find that noise level should be around $460\,nV/\sqrt{Hz}$ at 0.05 Hz. Our reference puts out about $708\,nV/\sqrt{Hz}$ at this frequency. However, a substantial part of this measurement ($270\,\mathrm{nV}/\sqrt{\mathrm{Hz}}$) might be due to the amplifier's input noise.

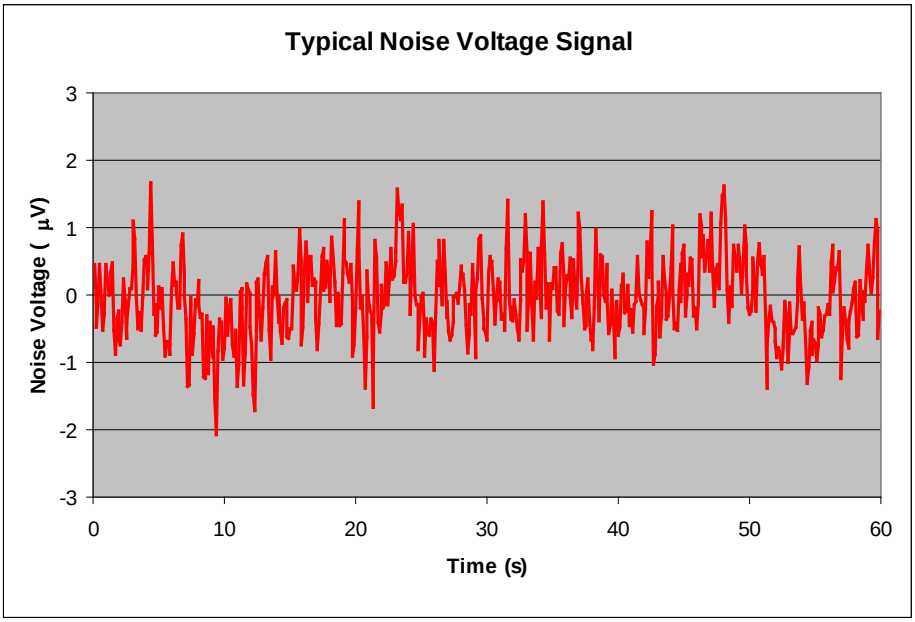

Figure 14. Raw noise signature from the LTZ1000

Next, we measured the voltage noise across the current sensing resistor. A spool of copper wire was used to simulate the bias coils. We calculated the voltage noise as described above and then we converted it to current noise by dividing through by 50Ω. The results of one such measurement are shown in Figure 16 (below). We found that our supply has roughly $16\,nA/\sqrt{Hz}$ at 0.05 Hz. As much as $2.5\,nA/\sqrt{Hz}$ of this noise may be due to the intrinsic noise mechanisms of the resistor itself. Assuming that we can construct perfectly stable coils, these values give us a magnetic field noise of around $1.1\times10^{-10}\,G/\sqrt{Hz}$ at the modulation frequency.

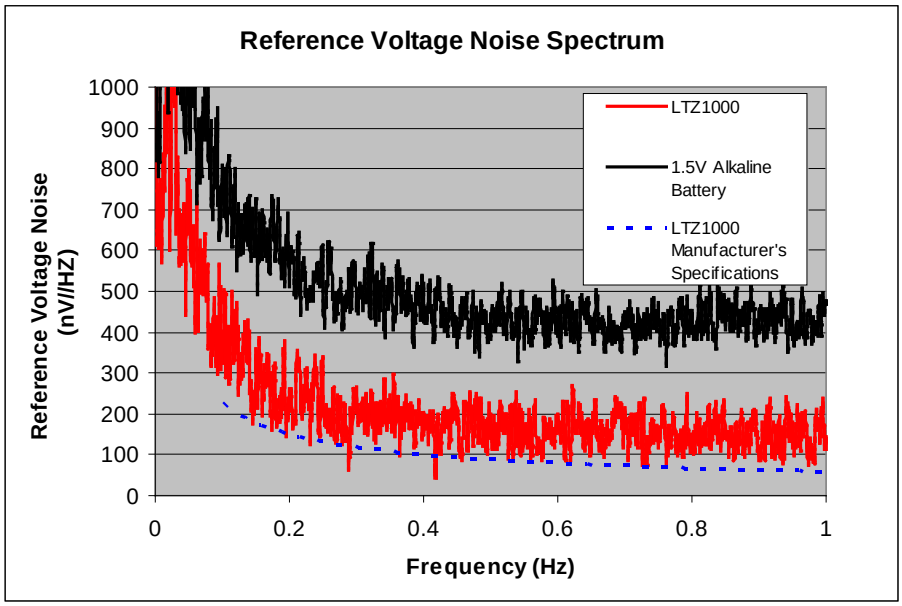

Figure 15. Noise spectrum of our reference circuit compared to an alkaline battery and the manufacturer's specifications.

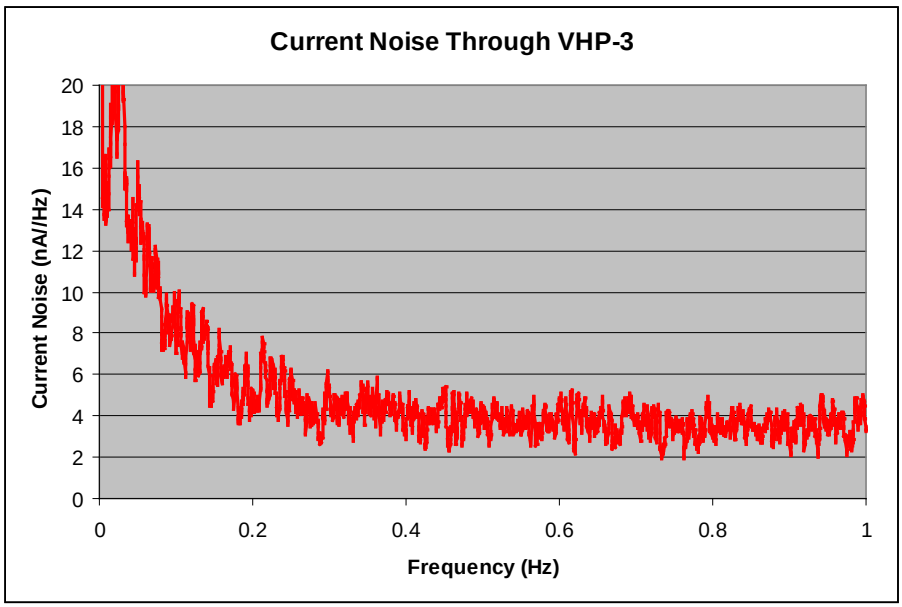

Figure 16. Noise spectrum of the current supply circuit as measured across the current sensing resistor.

Summary

The results show that our current supply is sufficiently stable to allow an EDM measurement of the desired precision. As it stands, the current supply can source a 140 mA current with $16\,nA/\sqrt{Hz}$ of noise at the modulation frequency of 0.05 Hz. This would correspond to a magnetic field noise of $1.14\times10^{-10}\,\mathrm{G}/\sqrt{\mathrm{Hz}}$ at this frequency. As much as $6\,\mathrm{nA}/\sqrt{\mathrm{Hz}}$ of the current noise might be attributed to voltage noise introduced by the inputs of the SR560 low-noise amplifier and by the intrinsic noise mechanisms present in the current sensing resistor. Assuming we can build sufficiently stable field coils, the desired magnetic field noise level of $8.7\times10^{-10}\,G/\sqrt{Hz}$ at 0.05 Hz should be achievable. However, we found that our supply is not as quiet as the original Berkeley design and better noise levels should be viable. This might be achieved by improving the noise on the voltage reference and through better thermal insulation and electromagnetic shielding.

It is expected that if we were to achieve the manufacturer's noise rating for the LTZ1000 ($460\,nV/\sqrt{Hz}$), we could improve the current noise level by a factor of 2. In order to achieve this, we recommend replacing the metal film resistors that are presently installed for higher precision wire wound resistors. These were not used in the first place because they are unavailable in the storeroom and we believed that metal film resistors would be sufficiently accurate. We will also try to clean up any excess solder flux as this has been shown to promote leakage currents on the PC board[23]. If further precision is required, perhaps the circuit can be rebuilt on a custom-made PC board paying special attention to its thermal layout and avoiding leakage currents.

Further improvement might be achieved by increasing the resistance of the current sensing resistor R_f such that the noise in the reference voltage translates into smaller current fluctuations. Unfortunately, it would also increase the Johnson voltage noise in the resistor by a factor of $\sqrt{\mathrm{R_{f,\,new}}/50\Omega}$. This solution would also mean that supply would source a smaller current and the magnetic field coils would have to have more turns. The resulting change in size should be taken into account, so that it does not exceed the size of the vacuum can. Care must also be taken so that the coil resistance does not exceed the load capacity of the current supply.

Some improvements might be achieved by encasing the supply and the batteries in a single chassis to achieve better shielding. This would prevent noise pickup in all the connecting cables and ease thermal insulation of all the components.

Unwanted high frequency components were also seen at around 100 kHz. These were easily filtered out in our noise measurements, but were unexpected. The source of these oscillations should be found and corrected or at the very least their effect on the experiment should be analyzed. A simple solution might be to put a bypass capacitor across the terminals of the reference, but the effects of a capacitive load should be carefully studied.

In conclusion, we believe that the level of current noise that we achieved in our supply should be sufficient to perform the desired electron EDM measurement. However, this level of noise is close to the technical limit of this design and future experiments may find bias field noise to be a limiting factor.

References

[1] Christensen J H, Cronin J W, Fitch V L and Turlay R 1964 *Phys. Rev. Lett.* 13 138

[2] M. E. Pospelov and I. B. Khriplovich, Sov. J. Nucl. Phys. **53**, 638 (1991).

[3] I. B. Khriplovich and S. K. Lamoreaux, *CP Violation Without Strangeness* (Springer, New York, 1997).

[4] K.F. Smith *et al.*, Phys. Lett. B **234**, 191 (1990); I.S. Altarev *et al.*, Phys. Lett. B **276**, 242 (1992); J.P. Jacobs, W.M. Klipstein, S.K. Lamoreaux, B.R. Heckel, and E.N. Fortson, Phys. Rev. A **52**, 3521 (1995); D. Cho, K. Sangster, and E.A. Hinds, Phys. Rev. Lett. **63**, 2559 (1989); E.D. Commins, S.B. Ross, D. DeMille, and B.C. Regan, Phys. Rev. A **50**, 2960 (1994); S.A. Murthy, D. Krause, Z. L. Li, and L.R. Hunter, Phys. Rev. Lett. **63**, 965 (1989).

[5] Commins, Eugene D, et al. "New Limit on the Electron Electric Dipole Moment" Physical Review Letters 88 (7) 2002

[6] Sandars, P.G.H. "The electric dipole of an atom" 14 (3) 1965: 194-196

[7] J. D. Miller, R. A. Cline, and D. J. Heinzen. "Far-off Resonance Trapping of Atoms" Physical Review A **57** (1992): 4567

[8] For an example of generation of slow atomic beams using a 2-D MOT see: Diekmann, K., et al. "Two-dimensional Magneto-optical Trap as a Source of Slow Atoms" Physical Review A **58** (5) 1998: 3891-3895

[9] Chu, S., et al. "Three-dimensional viscous confinement and cooling of atoms by resonance radiation pressure". Physical Review Letters 55 (1985): 48

[10] Ross, S.B., Davis, J.R, and Dutra J."An extremely low noise, low cost, constant current supply." Review of Scientific Instruments vol. 64, 8 (1993): 2379-2381

[11] "BBG-180RT Datasheet". Milwaukee, WI: C&D Technologies Inc, Dynasty Division, 2005

[12] "LT1028 Datasheet". Milipitas, CA: Linear Technology Corporation, 1992

[13] "LTZ1000/LTZ1000A Datasheet". Milipitas, CA: Linear Technology Corporation, 1987

[14] Spreadbury, P.J. "The Ultra-Zener… Is it a portable replacement for the Weston cell?" Measurement Science and Technology 1 (1990): 687-690

[15] Kopp, G., Lawrence G., and Rottman, G. "Total Irradiance Monitor Design and On-Orbit Functionality". Laboratory for Atmospheric and Space Physics, University of Colorado. SPIE Proc. 5171-4, 2003

[16] "CERN SL-PO Standards Laboratory Homepage" Geneva, Switzerland: European Organization for Nuclear Research. Last updated 08/2001 Visited 04/2005 URL: http://sl.web.cern.ch/SL/Pogroup/POsl.htm

[17] "2N2219A Datasheet" Watertown, MA: Microsemi Corporation, 1998

[18] "VHP-3, VHP-4, and VPR 247 Datasheet". Malvern, PA: Vishay Intertechnology Inc, 2005

[19] Lee, Mitchell. "Application Note 82: Understading and Applying Voltage References". Milipitas, CA: Linear Technology Corporation, 1999

[20] Pickering, John R. "United States Patent 5,369,245: Method and apparatus for conditioning an electronic component having a characteristic subject to variation with temperature". Alderford, Great Britain: 1994

[21] For a discussion of noise in passive components see: Ott, Henry. "Noise Reduction Techniques in Electronic Systems" New York: John Wiley & Sons, 1998

[22] "Model SR560 Low-Noise Preamplifier User's Manual" Sunnyvale, CA: Stanford Research Systems, 2004

[23] See reference 14 page 5

Appendix A: Final Construction Notes

Voltage Reference Circuit

This circuit takes up the majority of the circuit board. It is constructed using light green wire. The most visible components are a light blue electrolytic capacitor, which is not in the circuit diagram shown in Figure 10 and is one of two capacitors used to filter the power supply, the LT1013 dual op-amp, which is in a DIP package, and the LTZ1000 Ultra-Zener reference, which is a metal can with 8 legs. The LTZ1000 will get hot and should not be heatsunk, as it has a heating element inside and is supposed to operate at high temperature. Because it is designed to operate at elevated temperatures, the LTZ1000 should be allowed to warm-up and stabilize for at least 10 minutes

This circuit must be externally powered by a 12V battery. For this purpose there is a 4-pin connector on the current source chassis. The battery must be connected in such a way that it is isolated from earth ground. In particular, the positive terminal should be connected to pin 1, the negative terminal should be connected to pins 2 and 4, and neither terminal should be connected to ground. This guarantees that the current return from the heating element (which is noisy) does not meet the current return from the voltage reference until the last possible moment. The heating element on the LTZ1000 can draw a significant current and as such the battery charge should be checked after extended operation.

The output of this circuit is hardwired directly to the appropriate terminals on the current supply circuit. The reference voltage comes out via a black cable from pin 7 of the LTZ1000 (negative terminal) and a red cable from pin 3 of the LTZ1000 (positive terminal). While the wire from pin 7 goes to a switch on the chassis (S1 in Figure 7) before connecting into the current supply circuit, the wire from pin 3 is connected directly into the current supply circuit.

Unlike the mercury cell used in the Berkeley paper, the reference circuit must be turned on before turning on the remaining circuitry. There is no switch included for this and it is assumed that the user will do this by using the switch on one of the battery boxes that we have in the lab.

Current Supply Circuit

This circuit is built on along the edge of the board using dark green wire. It has a large Vishay resistor, which is in a large metal can and is heatsunk directly by a black heatsink. It also includes two dark blue electrolytic capacitors, which filter the power supply battery, as well as a large white film capacitor.

The circuit is powered by a C&D Technologies BBG-180RT 12 Volt Gell-Cell battery, which was purchased specifically for this purpose. As the sole source of current

in this circuit, it is optimized for continuous current drain. Although it is maintenance free, care should be taken maintain it well charged as low supply voltage will limit the load that the current source can supply. A rough method for estimating this limit was shown earlier.

The battery is connected directly to current supply circuit with the positive terminal going through a switch S2 and the negative terminal being connected to the chassis. Unlike the battery used to power the voltage reference (which should remain disconnected from earth ground at all times), the battery that powers the current supply should always be connected to earth ground (through the chassis). The grounded chassis then provides a shield from external interference.

The circuit has two switches, which are mounted on the chassis. The first (S1) connects the voltage reference circuit to the current supply circuit; the second (S2) connects current supply battery to the op-amp circuit. Normally, one would turn on S1 first, followed by S2. However, because the circuit has both positive and negative feedback, it can sometimes latch up at turn on. In this case, S2 should be turned off and back on.

The output of the current supply circuit is provided via Twinax connector on the chassis. It should then be fed to the load using the appropriate twin-axial cable to prevent noise pickup. The current supply should only be turned on when it connected to a load, so as not to risk damaging the circuitry.

Other Considerations

The chassis should remain closed so that there are no air currents running through it. These would cause instabilities in all the temperature sensitive components and would add noise to the system. To provide additional protection against thermal gradients, the chassis should be filled with Styrofoam peanuts.

Both chassis (including the tops) should be grounded to provide shielding against outside interference. This is also true for the braid of the cable leading the current to the load. Whenever possible, the current should be carried by a twisted pair configuration to prevent low-frequency noise pickup from stray magnetic fields.

Appendix B: Operation

How to use:

1.) Connect 12V battery to voltage reference circuit via 4-pin microphone connector on side panel of the chassis following the instructions as posted. Make sure the battery is floating and not connected to ground.
2.) Connect load to the Twinax connector on the front panel via twin-axial cable. The load resistance should not exceed 35Ω.
3.) Turn on switch on 12V battery box and allow the voltage reference to warm up for at least 10 minutes.
4.) Turn on Switch 1 to connect the voltage reference circuit to the current supply circuit.
5.) Turn on Switch 2 to connect the 12V Gel Cell to the current supply circuit.
6.) There should now be around 140mA of current going through the load. If this is not the case, toggle Switch 2 off, and then back on again.
7.) To shut down the supply, turn off Switch 2, then Switch 1, and finally turn off the battery supplying the voltage reference.